within 6 months after KT was estimated by the Kaplan-Meier method. Clinical and immunological factors were analyzed using Cox proportional hazard model. BKPyV-specific immune responses prior to and at 1 month after KT were compared using a mixed-linear regression test.

Results. Among 90 evaluable patients, 37% were female with a mean age + SD of 42 + 12 years. Sixty-four and 68 % received deceased-donor KT and induction immunosuppressive therapy, respectively. The cumulative incidence of BKPyV viruria within 6 months was 20%. In multivariate analysis, pre-transplant factors which were independently associated with BKPyV viruria were panel-reactive antibody of 11-50 % (HR 13.35; 95%CI, 1.926-92.590; P = 0.009), %natural killer (NK) cells (HR 1.26; 95%CI, 1.077-1.469; P = 0.004), and %VP1-specific NK cells (HR 1.25; 95%CI, 1.088-1.433; P = 0.002). Among those with BKPyV viruria, the mean %NK, %VP1-specific NK cells and %NKT cells at 1-month post-KT were significantly increased over time as compared to pre-KT (coefficient: 1.202; 95%CI, 0.033-2.371; P = 0.04), (coefficient: 2.602; 95%CI, 1.083-4.121; P = 0.001), and (coefficient: 0.199; 95%CI, 0.051-0.348; P = 0.008), respectively.

Conclusion. A presence and increasing proportion of NK, VP1-specific NK and NKT cells were observed among KT recipients who developed early and clinically significant BKPyV viruria in our cohort. Quantification of BKPyV-specific NK and NKT cell immune monitoring could potentially stratify those at risk of BKPyV viruria among KT recipients.

Disclosures. **All Authors**: No reported disclosures

1190. Dual-Plasmid Technology for Precision Genome Editing in Staphylococcus aureus

Jennifer Reish, BS[1]; Somrita Dey, PhD[1]; Kelsi Penewit, BS[2]; Stephen J. Salipante, MD PhD[2]; Andrew David. Berti, Pharm.D PhD[1]; [1]Wayne State University, Detroit, Michigan; [2]University of Washington, Seattle, Washington

Session: P-53. Microbial Pathogenesis

Background. Genetic manipulation of *Staphylococcus aureus* (both methicillin sensitive *S. aureus*, MSSA, and methicillin resistant *S. aureus*, MRSA) poses a technical challenge due to poor transformation efficiency, limited endogenous DNA repair activity, lineage-specific methylation patterns and intrinsic resistance to common selectable markers.

Methods. To address transformation efficiency we have optimized electrocompetent cell preparation and electroporation protocols for staphylococci. Further, we have improved a CRISPR counterselection platform that delivers a heterologous ssDNA recombinase and an inducible Cas9 endonuclease. When used for recombineering and counterselection, this strategy allows minimization of the number of elements necessary to transform in a single electroporation event. The Cas9 delivery platform has been modified to include a range of selectable markers including resistance to apramycin, erythromycin, kanamycin, nourseothricin, spectinomycin or trimethoprim.

Results. Overall electroporation efficiency increased by multiple orders of magnitude (> 100×) using the optimized cell preparation protocol. The CRISPR delivery platform can be stably maintained in a repressed state for multiple generations and induced with anhydrotetracycline. We have introduced targeted mutations in multiple loci using this system with an average turnaround time of 12 days.

Conclusion. This improved dual-plasmid CRISPR platform is robust and allows the investigator to rapidly and specifically alter the genomes of staphylococci. These tools will facilitate the study of how specific genetic polymorphisms contribute to various phenotypes in *S. aureus*, including the virulence of MRSA.

Disclosures. **All Authors**: No reported disclosures

1191. Evolution of Hepatitis C Virus Points to Postpartum Recovery of CD8+ T-Cell Selection Pressure

Stephanie Smith, MD[1]; Zhaohui Xu, PhD[1]; Christopher Walker, PhD[1]; Jonathan Honegger, MD[2]; [1]Nationwide Children's Hospital, Columbus, Ohio; [2]Nationwide Children's Hospital, The Ohio State University, Columbus, OH

Session: P-53. Microbial Pathogenesis

Background. In acute persisting hepatitis C virus (HCV) infection, brief control of viral replication can occur with onset of a cellular immune response but is eventually lost due to selection of viral variants with escape mutations in CD8 T cell epitopes or development of T cell exhaustion. In chronic infection, the CD8s targeting remaining intact epitopes are exhausted, viral levels are stable, and selection of new escape mutations is rare. Postpartum (PP), some chronically infected women experience a drop in viremia which we hypothesize is due to recovery of the CD8 response and will be associated with selection of de novo escape mutations as seen in acute persisting infection.

Methods. HCV genomic evolution was assessed in 2 women with different patterns of PP viral control through consecutive pregnancies. Subject M016 experienced > 2.5 $\log_{10}$ drops in viral loads after each pregnancy while M062 had stable viral levels (Table 1). Longitudinal viral genomes were assessed by Illumina sequencing of near full length PCR products of viral cDNA. Reads were initially aligned to a genotype reference and then iterative consensus sequences until deep coverage was achieved across the entire PCR amplicon. To identify potential CD8 escape mutations, amino acid substitutions were counted if their frequency increased from < 10% of reads peripartum to > 90% at follow up. We focused on the nonstructural region to avoid substitutions related to antibody selection pressure.

Viral Load Levels

Table 1: Viral load Levels

Subject	Peripartum 1st Pregnancy ($\log_{10}$)	3 months Postpartum 1st Pregnancy ($\log_{10}$)	Peripartum 2nd Pregnancy ($\log_{10}$)	3 months Postpartum 2nd Pregnancy ($\log_{10}$)
M016	5.91	1.88	5.77	3.08
M062	7.38	7.11	6.45	6.9

Results. M016 developed 3 nonsynonomous (NS) mutations after her 1st pregnancy and 1 more after her 2nd. Of these, 3 were directed away from the consensus amino acid sequence, and one differed from consensus at baseline and changed tangentially. M062 developed 1 NS mutation within a known class I epitope following her second pregnancy which was directed toward consensus for her genotype (Fig 1). All mutations occurred within predicted class I epitopes.

Nonsynonomous Substitutions in Nonstructural Region

Figure 1:

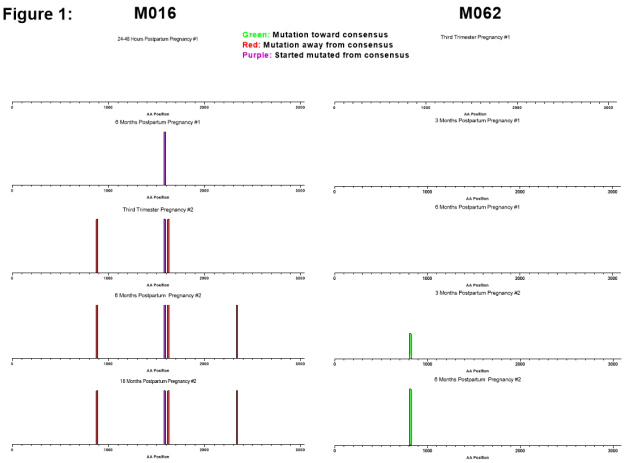

Conclusion. While these pilot data require verification in additional subjects, the observed emergence of non-synonymous mutations directed away from genotype consensus in viral class I epitopes of a woman with postpartum viral control but not in a women with stable viral levels support our hypothesis enhanced CD8 T cell selection pressure contribute to enhanced control of HCV replication after childbirth.

Disclosures. **All Authors**: No reported disclosures

1192. H-NS-like Proteins in Pseudomonas aeruginosa Coordinately Silence Intragenic and Antisense Transcription

Andrew M. Lippa, MD, PhD[1]; Michael J. Gebhardt, PhD[1]; Simon L. Dove, PhD[2]; [1]Boston Children's Hospital, Boston, Massachusetts; [2]Boston Children's Hospital/ Harvard Medical School, Boston, Massachusetts

Session: P-53. Microbial Pathogenesis

Background. The H-NS-like proteins MvaT and MvaU act coordinately as global repressors in *Pseudomonas aeruginosa* by binding to AT-rich regions of the chromosome, which include horizontally acquired genes and numerous virulence factors. Although cells can tolerate the loss of either protein, identifying their combined regulatory effects has been challenging because the loss of both proteins is lethal due to induction of the prophage Pf4 and subsequent superinfection of the cell. Although in other bacteria, H-NS promotes cellular fitness by inhibiting intragenic transcription from AT-rich target regions, preventing them from sequestering RNA polymerase, a role for MvaT and MvaU in repressing transcription from intragenic promoters has not been demonstrated.

Methods. Here we utilize a parental strain that cannot be infected by Pf4 phage to identify the combined MvaT and MvaU regulon. RNA-seq was utilized to identify genes differentially expressed in cells lacking MvaU or both MvaU and MvaT. ChIP-seq was utilized to identify genes directly regulated by MvaT and MvaU in wild-type cells. Further, ChIP-seq was performed in cells of the parental strain and cells lacking both MvaT and MvaU to map genome-wide σ^{70}-dependent promoters that were active in the presence or absence of both H-NS-like proteins.

Results. We demonstrate that the loss of both MvaT and MvaU, but not MvaU alone, leads to increased sense, antisense, and intragenic transcription from loci directly controlled by these proteins. We further show that the loss of MvaT and MvaU leads to a striking redistribution of RNA polymerase containing σ^{70} to those genomic regions vacated by these proteins.

Loss of MvaT and MvaU causes global changes in gene expression

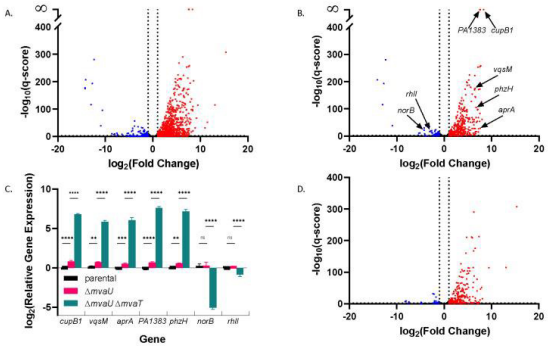

A. RNA-seq was performed in cells lacking *pilY1* (parental) and in cells also lacking *mvaT* and *mvaU*. A volcano plot demonstrates transcripts with statistically significant differential expression in *ΔmvaT ΔmvaU* vs parental (q<0.01, horizonal dotted line) and absolute value of fold change ≥2 (lateral of vertical dotted lines). Red and blue points indicate transcripts with increased and decreased abundance in *ΔmvaT ΔmvaU* relative to the parental, respectively. Black points indicate transcripts whose differential expression does not meet statistical significance or whose fold change was less <2.
B. A volcano plot of only the coding (sense) transcripts for annotated genes is shown.
C. Candidate genes, indicated in the volcano plot (B), were validated by qRT-PCR.
*p<0.05, **p<0.01, ***p<0.001, ***p<0.0001
D. A volcano plot of only transcripts antisense to annotated genes is shown.

Loss of MvaT and MvaU results in increased sense and antisense transcription

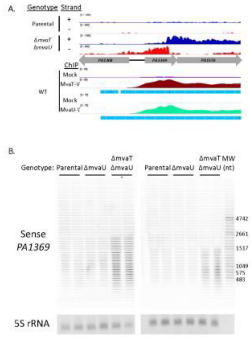

Loss of MvaT and MvaU results in increased sense- and antisense transcription.
A. RNA-seq was performed in cells lacking *pilY1* (parental, *mvaU*$^{+}$ *mvaT*$^{+}$) and in cells also lacking *mvaT* and *mvaU*. Reads are showed aligned to plus (blue) and minus (red) strands, scaled equally among plus and minus stranded reads, respectively. A representative region showing both sense (blue) and antisense (red) transcripts only in cells lacking *mvaT* and *mvaU* is shown for the *PA1369* gene, an annotated conserved hypothetical protein. ChIP-seq performed in strains that are wild-type with exception of an in-frame epitope tag on either *mvaT* (MvaT-V) or *mvaU* (MvaU-V) demonstrate MvaT and MvaU occupancy in the region of increased sense and antisense transcripts in the *ΔmvaT ΔmvaU* strain. RNA-seq and both MvaT-V and MvaU-V ChIP-seq were performed in biologic triplicate. Representative tracks for a single replicate are shown.
B. A Northern blot was performed with RNA from cells with the parental genotype, cells lacking *mvaU* only, and cells lacking both *mvaU* and *mvaT*. The membrane was hybridized with probes that bind to the coding strand (sense) or non-coding strand (antisense) of *PA1369*. Increases in both sense and antisense transcripts of apparently different size are seen only when cells lack both *mvaT* and *mvaU*. 5S rRNA is shown as a loading control. Two biological replicates for each strain are shown.

Loss of both MvaT and MvaU results in genome-wide redistribution of RNA polymerase

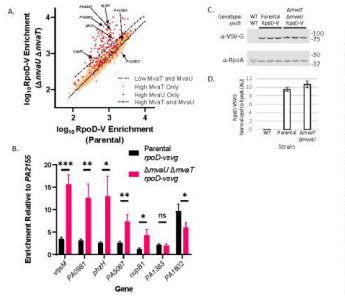

Loss of MvaT and MvaU results in redistribution of RNA polymerase subunit σ^{70} genome-wide.
A. RpoD-V enrichment scores were ascertained summed across each annotated gene. Each point represents the log RpoD-V enrichment for an annotated gene in the parental strain (x coordinate) and *ΔmvaU ΔmvaT* strain (y coordinate). Genes whose association is unchanged by deletion of *mvaT* and *mvaU* will follow a y=x distribution. Plotted genes were subdivided by enrichment for MvaT-V and MvaU-V: not enriched for MvaT-V and MvaU-V (peach), enriched for MvaT-V but not MvaU-V (green), enriched for MvaU-V but not MvaT-V (blue), and enriched for both MvaT-V and MvaU-V (red). Comparison of linear regression for the dual-enriched (high MvaT and MvaU, dot-dash) and dual-unenriched (low MvaT and MvaU, dashed) demonstrates a statistically significant difference in y-intercept (p<0.0001) for the two trendlines.
B. Candidate genes were evaluated for enrichment of RpoD-V by ChIP-qPCR in the parental (black) and *ΔmvaU ΔmvaT* strain (magenta). Error bars represent the standard deviation of a biological triplicate performed in technical triplicate. Significance was determined using the two-stage linear step-up procedure of Benjamini, Krieger and Yekutieli, with Q = 1% and without the assumption of consistent standard deviation.
C. Protein was isolated from cells of the parental strain with epitope-tagged RpoD-V and a similar strain also lacking *mvaT* and *mvaU*, each grown in biological triplicate. Quantitative western blot was performed using antibodies against the VSVG epitope tag on RpoD and a loading control (α subunit of RNA polymerase). Protein isolated from wild-type cells was loaded as a single negative control lane.
D. VSVG signal is shown normalized to the loading control.
*p≤0.05, **p<0.01, ***p<0.001, ***p<0.0001

Conclusion. Our findings suggest that the ability of H-NS-like proteins to repress intragenic transcription is a universal function of these proteins and describe a second mechanism by which MvaT and MvaU may contribute to the growth of *P. aeruginosa*.

Disclosures. **All Authors**: No reported disclosures

1193. Human Transcriptomic Analysis of Periprosthetic Joint Infection

Thao Masters, PhD[1]; Aditya Bhagwate, MS[1]; Mrunal Dehankar, MS[1]; Kerryl Greenwood-Quaintance, MS[1]; Matthew P. Abdel, MD[2]; Robin Patel, MD[1]; Robin Patel, MD[1]; [1]Mayo Clinic, Rochester, Minnesota; [2]Mayo Clinic Rochester, Rochester, Minnesota

Session: P-53. Microbial Pathogenesis

Background. Periprosthetic joint infection (PJI), a devastating complication of total joint replacement, is of incompletely understood pathogenesis and may sometimes be challenging to clinically distinguish from other causes of arthroplasty failure.

Methods. We characterized human gene expression in 93 specimens derived from surfaces of resected arthroplasties, comparing transcriptomes of subjects with infection- *versus* non-infection-associated arthroplasty failure.

Results. Differential gene expression analysis confirmed the association of 28 previously investigated biomarkers with PJI- bactericidal/permeability increasing protein (BPI), cathelicidin antimicrobial peptide (CAMP), chemokines CCL3, CCL4, and CXCL2, colony stimulating factor 2 receptor (CSF2RB), colony stimulating factor 3 (CSF3), alpha-defensin (DEFA4), receptor CD64B, intercellular adhesion molecule 1 (ICAM1), IFNG, IL13RA2, IL17D, IL1A, IL1B, IL1RN, IL2RA, IL2RG, IL5RA, IL6, IL8, lipopolysaccharide binding protein (LBP), lipocalin (LCN2), lactate dehydrogenase C (LDHC), lactotransferrin (LTF), matrix metallopeptidase 3 (MMP3), peptidase inhibitor 3 (PI3), and vascular endothelial growth factor A (VEGFA), as well as identified three novel molecules with diagnostic potential for detection of PJI- chemokine CCL20, coagulation factor VII (F7), B cell receptor FCRL4. Comparative analysis of infections caused by *staphylococcal versus* non-*staphylococcal* and *Staphylococcus aureus versus Staphylococcus epidermidis* showed significant elevated expression of IL13, IL17D, and metalloprotease protein MMP3 in *staphylococcocal* infections, and increased expression of IL1B, IL8, and platelet factor PF4V1 in *S. aureus* infections. Pathway analysis of over-presented genes suggested activation of host immune response and cellular maintenance and repair functions in response to invasion of infectious agents.

Conclusion. Our study provides new potential targets for diagnosis of PJI and targets for differentiation of PJI-associated infectious agents.

Disclosures. Matthew P. Abdel, MD, Dr. Abdel receives royalties from Stryker on certain hip and knee products, and is a paid consultant for Stryker. (Consultant) Robin Patel, MD, Accelerate Diagnostics (Grant/Research Support)CD Diagnostics (Grant/Research Support)Contrafect (Grant/Research Support)Curetis (Consultant) GenMark Diagnostics (Consultant)Heraeus Medical (Consultant)Hutchison Biofilm Medical Solutions (Grant/Research Support)Merck (Grant/Research Support)Next Gen Diagnostics (Consultant)PathoQuest (Consultant)Qvella (Consultant)Samsung (Other Financial or Material Support, Dr. Patel has a patent on Bordetella pertussis/parapertussis PCR issued, a patent on a device/method for sonication with royalties paid by Samsung to Mayo Clinic, and a patent on an anti-biofilm substance issued.) Selux Dx (Consultant)Shionogi (Grant/Research Support)Specific Technologies (Consultant)

1194. Identification and Characterization of Extracellular Inducers of Persistence in Staphylococcus epidermidis and Staphylococcus aureus

Danni Y. Habtu, DO, MS[1]; Neal Chamberlain, PhD[2]; Elyse Curry, MS[3]; Ryan Hart, MS[4]; [1]Wayne State University, Royal Oak, Michigan; [2]A.T. Still University of Health Sciences/KCOM/MOSDOH, Kirksville, Missouri; [3]A.T. Still University of Health Sciences/KCOM, Kirksvillle, Missouri; [4]University of California- Davis, Davis, California

Elyse C. Curry, Ryan G. Hart, Danni Y. Habtu and Neal R. Chamberlain

Session: P-53. Microbial Pathogenesis

Background. This study describes the identification and partial characterization of persistence inducing factors (PIF) from *Staphylococcus aureus* (*S. aureus*) and *Staphylococcus epidermidis* (*S. epidermidis*). Persistence is an epigenetic process that results in tolerance of bacterial cells to antibiotic treatment, which can result in chronic human infections.

Methods. Others have demonstrated a significant increase in persister numbers during mid-log phase. Inducers of this mid-log increase have yet to be identified in staphylococci. Optical density at 600 nm (OD_{600}) was used instead of time to determine when persister numbers increased during logarithmic growth. Concentrated culture filtrates (CCF) from *S. epidermidis* RP62A and *S. aureus* SH1000 were obtained at various OD_{600}'s and following incubation at 16 h. The CCF's were used to develop a persistence inducing factor (PIF) assay. The PIF assay was used to partially characterize PIF from *S. epidermidis* RP62A and *S. aureus* SH1000 for relative molecular weight, temperature and protease sensitivity and inter-species communications.

Results. Optimal OD_{600}'s for the *S. epidermidis* RP62A and *S. aureus* SH1000 PIF assays were 2.0 and 0.5, respectively. The highest PIF activity for both species was from CCF following incubation overnight (16 h). *S. epidermidis* RP62A's PIF activity was decreased by storage at 4° C (2 weeks or longer) but not following incubation at 20° C (16 h), 37° C (1 h) or 100° C (15 min). *S. aureus* SH1000's PIF activity was decreased following storage at 4° C (2 week or longer) and after boiling at 100°C for 5 min but not after incubation at 37° C (1 h). PIF activity from both species was less than 3,000 Mrr. Proteinase-K treatment of *S. aureus* SH1000 PIF decreased activity but did not decrease PIF activity of *S. epidermidis* RP62A. PIF from *S. epidermidis* RP62A did not increase persister numbers when used to treat *S. aureus* SH1000 cells nor did PIF from *S. aureus* SH1000 increase persister numbers in *S. epidermidis* RP62A cells.

Conclusion. Previous attempts to discover PIF's for staphylococcal species were unsuccessful due to the time-based means used to identify mid-log. Both staphylococcal species appear to produce unique, extracellular, low-molecular-weight inducers of persistence (PIF) when assayed using an OD_{600}-based PIF assay.

Disclosures. **All Authors**: No reported disclosures

1195. Influence of Histoplasma capsulatum Infection on Endothelin-1 mRNA Gene Expression in Bone Marrow Derived Macrophages

Eloho Ajayi, MD[1]; George S. Deepe, Jr, MD[2]; William R. Buesing, n/a[1]; [1]University of Cincinnati, College of Medicine, Cincinnati, Ohio; [2]University of Cincinnati, Cincinnati, Ohio

Session: P-53. Microbial Pathogenesis

Background. Endothelin-1 (ET-1) is increasingly recognized as an immune modulator; it exerts a pro-inflammatory effect by increasing the release of cytokines like interferon gamma. ET-1 is secreted by a variety of cells such as macrophages, neurons and endothelial cells. Activation of the endothelin system has been implicated